INPROVEMENT OF FIELD EMISSION PROPERTIES OF PbS THIN FILMS BY AMORPHOUS CARBON COATING

S. Jana[1], **D. Banerjee**[2], **B. Kamaliya**[3], **K.K. Chattopadhyay**[1,2]

[1] Thin Films and Nanoscience Laboratory,
   Department of Physics, Jadavpur University, Kolkata-700032, India
   E-mail: Sananda.juphy@gmail.com

[2] School of Material Science and Nanotechnology,
   Jadavpur University, Kolkata 700032, India

[3] Applied Physics Department,
   M.S. University of Baroda, Vadodara, India

Lead sulfide (PbS) nanocrystalline thin films were synthesized at room temperature via chemical bath deposition on both silicon and glass substrates and coated with amorphous carbon of different thickness by varying deposition time in plasma enhanced chemical vapor deposition technique. The as prepared samples were characterized by X-ray diffraction (XRD), field emission scanning electron microscope (FESEM) and atomic force microscope (AFM). XRD study reveals that coating of amorphous carbon does not change the crystal structure of PbS. From FESEM images it is seen that the average size of PbS nanoparticle does not exceed 100 nm, though sometomes small cubic particles agglomerated to form bigger particles. The coating of amorphous carbon can be clearly visible by the FESEM as well as from AFM micrographs. Field emission study show a significant betterment for the carbon coated sample as compared to the pure PbS. The effect of inter-electrode distance on the field emission characteristics of best field emitting sample has been studied for three different inter-electrode distances.

1. INTRODUCTION

Recently different carbon and carbon related materials have taken the worldwide attention regarding both the research and industrial activities. Carbon is really a unique material in the sense that it can exists in numberless forms belonging to both amorphous and crystalline class and thus can be applied in different technological. For instance, crystalline diamond is one of the hardest materials and thus can be applied in different mechanical and thermal applications [1-3] or crystalline carbon nanotube (CNT) or nanofiber (CNF) primarily due to their high aspect ratio and unique electronic configuration have found their application in field emission display (FED), gas storage device, drug delivery reagent and in many others [4-7]. Also different amorphous phase of carbon such as amorphous carbon, tetrahedral amorphous carbon, diamond like carbon,

carbon soot all have found their potentials in various field like field emission display [8, 9], mechanical application [10], tribological field [11], solar cell [12], etc. Apart from that, different amorphous carbons (a-carbon) have found its application in optical windows, magnetic storage discs, car parts, biomedical coatings and in micro-electromechanical devices (MEMS). There is another very important use of a-carbons and that is in different coating industries [13-15]. For instance, a-carbon coating may be used in order to obtain hydrophobic surface [16]. Recently Huang et al. reported an improved field emission characteristic of a-carbon coated copper nanowire compared to pure a-carbon [17]. There are also similar reports of enhanced electron emission from certain material when it is coated with a-carbon as compared to either of the pure material [18, 19]. Following these results here in this work we have first synthesized thin films of cubic shaped PbS nanoparticles and coated it with a-carbon of different thickness by direct current plasma enhanced chemical vapor deposition (dc-PECVD) and studied the changes of crystalline, structural and field emission properties of PbS thin films, caused by the a-carbon coating. PbS is one of the most important IV-VI semiconductors because of its larger exciton Bohr radius and relatively narrow band gap which can be blue shifted from the near infrared (IR) to the visible region by forming nanocrystallites [20]. Consequently, PbS nanoparticles have exhibited novel and excellent optical and electrical properties and applications in nonlinear optical devices such as, IR detectors [21], display devices [22], Pb^{2+} ion selective sensors [23] and solar control coatings [24]. PbS nanoparticles can be used in electroluminescent devices such as light emitting diodes and in optical devices such as optical switches due to their exceptional third order nonlinear optical properties [25]. But there is no report regarding the field electron emission from lead sulfide and also, though PbS nanoparticles show luminescence, but this is mostly in IR region [26]. Here for the first time we have reported the field emission from PbS nanocrystal and also shown that the field emission from such material can be enhanced significantly by coating it with a thin layer of a-carbon without sacrificing much, regarding crystallinity and optical gap of such material.

2. EXPERIMENTAL

2.1 Preparation of cubic PbS nanoparticle

Preparation of PbS nanoparticle via CBD techniques was described elsewhere in detail [27]. Briefly speaking, a solution, prepared by taking 4.98 mmol of lead acetate and 0.02 mol of sodium hydroxide (NaOH) dissolved in 30 ml of deionized water, was added in 150 ml deionized water. After 10 minute's continuous stirring, 11.82 mmol of thiourea (NH_2CSNH_2) dissolved in 20 ml deionized water was added to it, while the solution was continuously stirred. The whole process was carried out in the room temperature. Cleaned glass and stainless steel substrates were dipped into the solution for the deposition of the films by the CBD method. Before deposition, glass substrates were cleaned by mild soap solution and washed thoroughly in distilled water and in boiling water. Finally, they were ultrasonically cleaned in acetone for 15 min. The time of deposition was about 1 h. The CBD of PbS thin films is based on the decomposition of NH_2CSNH_2 in an alkaline solution containing a lead salt. This is achieved by controlled precipitation of PbS in the reaction bath. As

the solubility product of PbS is very small, the precipitation is controlled by controlling the concentration of free Pb^{++} ions in them chemical bath. This is done by using a suitable complexing agent, which releases a small concentration of ions, according to the complex-ion-dissociation equilibrium. In this case, NaOH is used as the complexing agent. The chemical reaction for the deposition of PbS by CBD is given by

$$SC(NH_2)_2 + OH^{-1} = CH_2N_2 + H_2O + HS$$
$$HS^- + OH^{-1} = H_2O + S^2$$
$$Pb^{2+} + S^{2-} = PbS$$
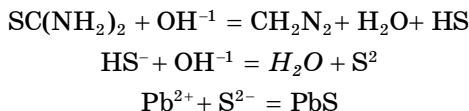
When the ionic product of Pb^{++} and S^{--} exceeds the solubility product of PbS, the precipitation of PbS can occur either in sol or on the surface of the substrates.

2.2 Coating of cubic PbS nanoparticle with amorphous carbon

The as synthesized PbS thin film were coated with amorphous carbon by dc-PECVD method. In a typical experiment a set of PbS thin film deposited on both silicon and glass substrates were transferred to PECVD chamber and placed on a grounded electrode. Then a base pressure of 10^{-6} mbar was achieved with the help of a rotary and diffusion pump. Acetylene was introduced as carbon feedstock that raised the final pressure of the CVD chamber to 0.5 mbar. A dc voltage 2 kV was applied through other electrode. No additional temperature was applied. The deposition time was varied from 0, 0.5, 2, 4 and 6 minutes in order to vary the thickness of the coating accordingly.

The as prepared samples were characterized by X-ray diffraction spectrometer (XRD Bruker D8 Advance), field emission scanning electron microscope (FESEM, Hitachi, S-4800), atomic force microscopy (AFM NT-MDT, Solver Pro.) and by our home made high vacuum field electron emission set up.

3. RESULTS AND DISCUSSIONS

3.1   XRD analysis

The crystalline structure of the as prepared samples has been studied by XRD using a diffractometer with CuK_α radiation (λ = 0.15406 nm) operating at 40 kV, 40 mA with a normal θ-2θ scanning. Fig. 1 shows a typical XRD pattern of amorphous carbon coated PbS thin films. It is seen that there are several diffraction peaks at 2θ values of 26.02, 30.25, 43.1, 51.06 and 53.47. These are assigned to the diffraction lines produced by (111), (200), (220), (311) and (222) planes of the face-centered-cubic (fcc) rock-salt structure of PbS [27]. There is no peak that corresponds to post deposited carbon as expected. It is clearly seen that the intensity of the peaks decreased with longer deposition time of amorphous carbon.

3.2   FESEM analysis

Fig. 2 a shows the FESEM image of pure PbS thin film without coating. It can be observed very clearly that PbS particles deposited are cubic in shapes with average dimension around 100 nm. Fig. 2 b shows the FESEM image of the coated sample where, a-carbon was deposited for 2 minute. It is clearly seen that the cubic PbS nanoparticles are covered with a-carbon. But the

covering is incomplete as the deposition time was too short. For the sample with deposition time 4 (Fig. 2 c) and 6 minute (Fig. 2 d), it is clearly seen that a layer of a-carbon has been deposited over PbS thin films. The deposition of this amorphous carbon is basically a cluster deposition without formation of any definite structures.
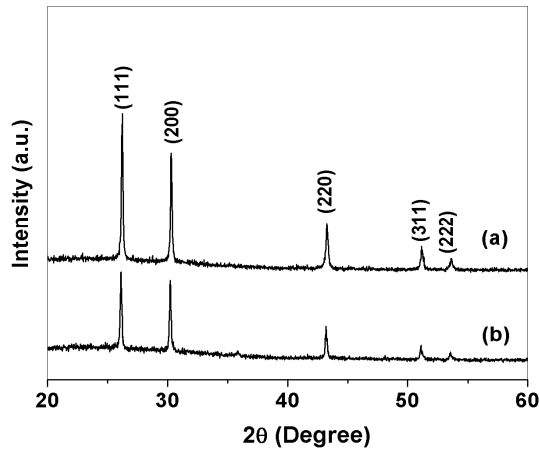
Fig. 1 − *XRD patterns of coated PbS samples where amorphous carbon was deposited for (a) 0.5 and (b) 2 minute*
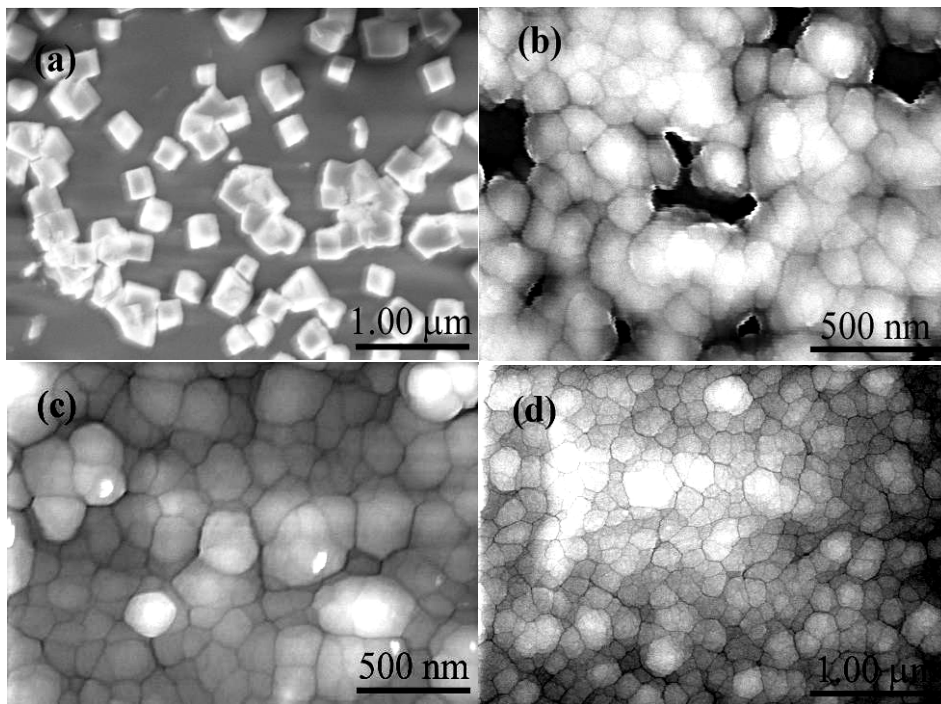
Fig. 2 − *FESEM images of (a) uncoated PbS nanoparticles, coated PbS samples with carbon deposition time of (b) 2, (c) 4, and (d) 6 minute*

3.2 AFM analysis

AFM imaging was used to analyze the surface topography of the uncoated and carbon coated samples recorded in semi-contact mode. Typical AFM image of uncoated PbS film is shown in Fig. 3 a. From size versus number of particle histogram it was found that the average grain size was ~ 50 nm. Fig. 3 b-c shows 2D AFM images and their corresponding histogram of the
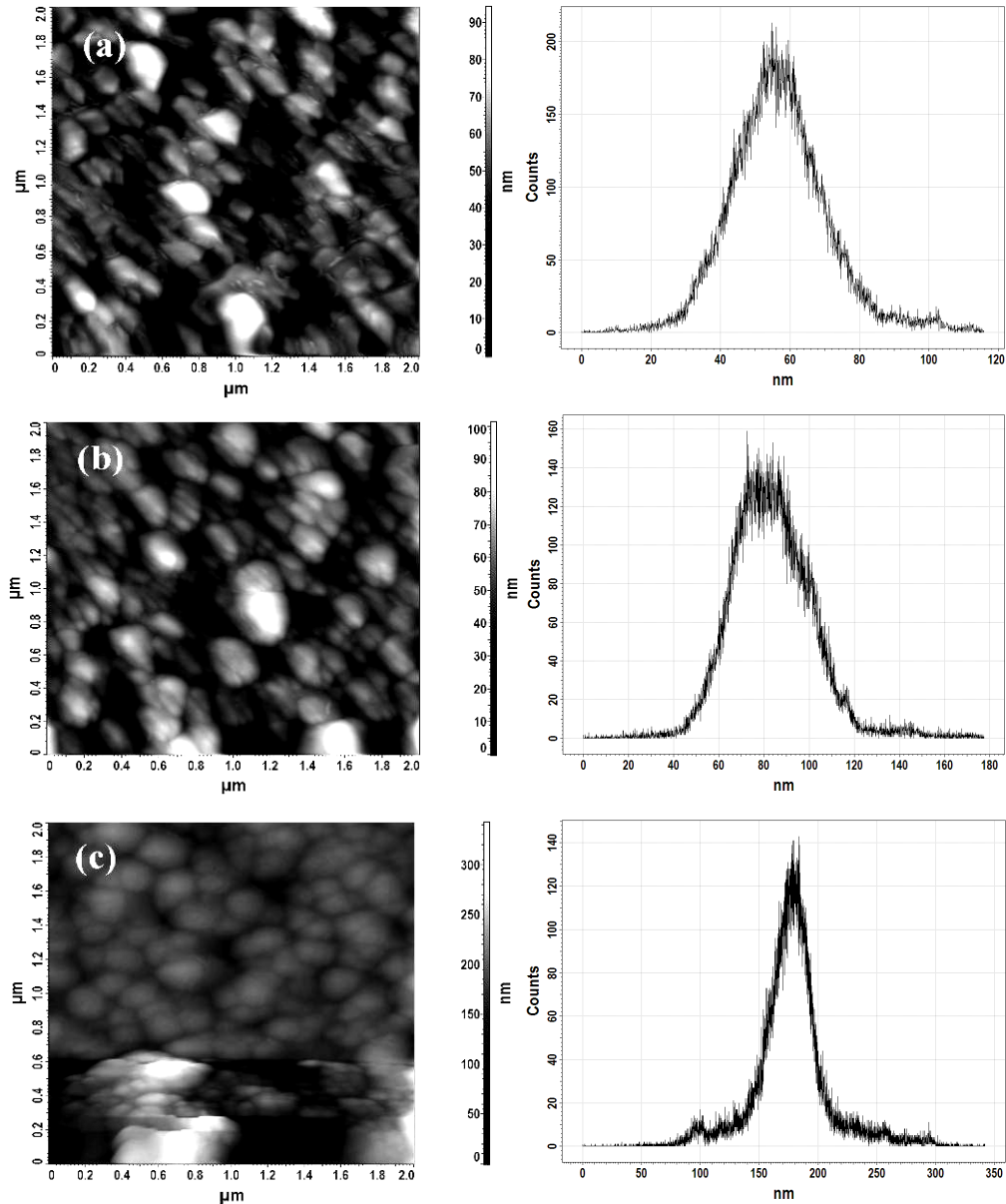
Fig. 3 − *AFM images with corresponding histograms of sample (a) uncoated PbS, coated PbS with (b) 2 minute and (c) 6 minute of carbon deposition time*

PbS thin films with 2 min and 6 min of carbon deposition time. It is seen that the roughness as well as particle size of the coated samples monotonically increases with a-carbon deposition time. The corresponding effects are manifested in the field emission studies discussed in section 3.4. As we can see that the deposition is basically cluster deposition it is vary expected that with time the cluster size became bigger and so the roughness increases.

3.3   Field emission study

The field emission study has been carried out in our home-made high vacuum field emission set up by using a diode configuration consisting of a cathode (the film under test) and a stainless steel tip anode (conical shape with a 1mm tip diameter). The measurements were performed at a base pressure of $\sim 10^{-7}$ mbar. The tip-sample distance was made adjustable to a few hundred micrometers by means of a micrometer screw. It was confirmed that there was no discharge and the current observed due to cold field emission of electron. The macroscopic applied electric field can be obtained by dividing the applied voltage by the inter electrode distance. Theoretically, the emission current and the macroscopic electric field related to each other by the well known Fowler-Nordheim equation [28],

$$I = Aat_F^{-2}\varphi^{-1}(\beta E)^2 \exp\{-bv_F\varphi^{3/2} / \beta E\} \tag{1}$$

Where A is the effective emission area, β is the enhancement factor, t_F, v_F are the values of special field emission elliptic function for a particular barrier height φ [29], a and b are respectively the first and second Fowler-Nordheim (F-N) constants having values $a = 1.541434 \cdot 10^{-6}$ AeV·V^{-2} and $b = 6.83089 \cdot 10^9$ eV$^{-3/2}V \cdot m^{-1}$. The F-N equation when simplified takes the form as,

$$\ln\{J / E^2\} = \ln\{t_F^{-2}a\varphi^{-1}\beta^2\} - [\{v_Fb\varphi^{3/2}\beta^{-1}\} / E] \tag{2}$$

where $J = I/A$ is the macroscopic current density. Hence plot of $\ln\{J/E^2\}$ vs. $1/E$ should be a straight line and its slope and intercept gives the valuable information about the enhancement factor, local work function etc. An experimental F-N plot has been modeled which can be expressed as,

$$\ln\{J / E^2\} = \ln\{ra\varphi^{-1}\beta^2\} - [\{sb\varphi^{3/2}\beta^{-1}\} / E] \tag{3}$$

Where r and s are respectively the intercept and slope correction factors. Typically, the value of s is nearly unity but r may have values, which may be as high as 100 and even greater [30]. The experimental *J-E* curve for the uncoated and carbon coated PbS samples has been shown in Fig. 4a. It is seen that pure PbS is far inferior field emitter compared to the coated PbS sample with carbon deposition time of 4 minute. That means that the coating of carbon helps the PbS to behave as field emitter keeping their crystalinity or optical bandgap remains almost same. The linear nature of the F-N plots shown in Fig. 4b suggests that the electrons are emitted due to cold field emission. It can be mentioned that for the determination of the turn-on field there exists no unique dentition. Different workers have defined it in different ways [31]. The turn-on field, which we define as the field where the current density increases by a significant jump and takes the

value 200 $\mu A/cm^2$, are found to be 18.22 and 3.1 V/μm for the uncoated and carbon coated PbS samples respectively. Also we computed enhancement factor obtained from the slope (m) of the F-N plots by using $\beta = -b\varphi^{3/2}/m$ and it is estimated to be 1930 and 12745 for the uncoated and coated PbS respectively. It can be seen that the field emission properties of the coated sample has been considerably enhanced. It is worthy to note here that the underlying PbS coating plays an important role in the field emission properties of the coated sample.
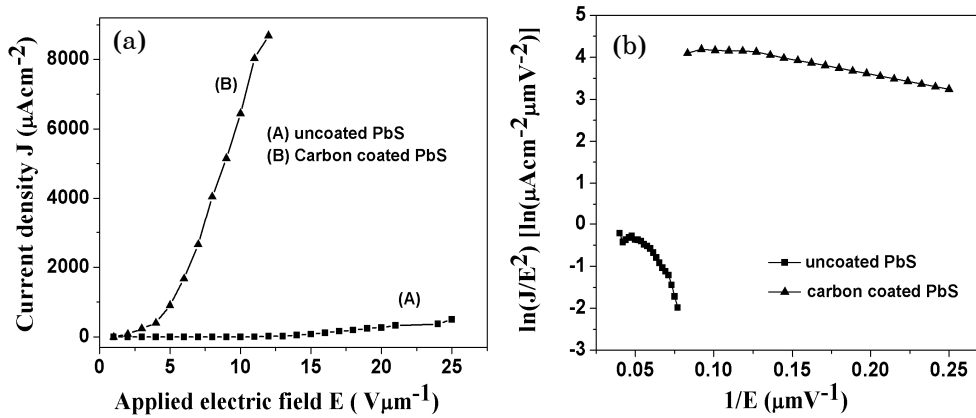
Fig. 4 − Plot of emission current density (J) versus macroscopic field (E) of uncoated and coated PbS films (carbon deposition time 4 minute) (a); and corresponding F-N plot (b)
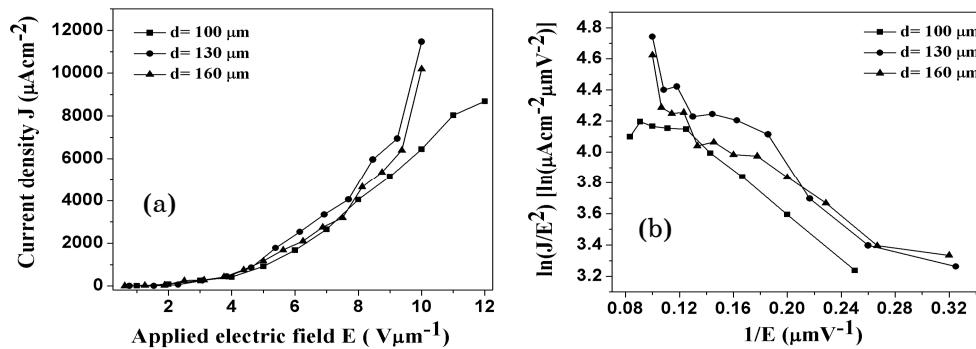
Fig. 5 − Plot of emission current density (J) versus macroscopic field (E) of coated PbS films (carbon deposition time 4 minute) for three different inter-electrode distance (a); and corresponding F-N plot (b)

The as synthesized PbS thin film has a sheet resistance of the order of several kΩ, so when PbS thin film is coated with a-carbon the higher concentration of electrons will enhance the electrical conductivity of the system because the greater supply of electrons and that in turn enhance the emission of electron into the vacuum. Also the underlying PbS particles enhanced the roughness of the coated films which is favorable for the enhanced emission. Similar result has been obtained by Huang et al. for their

amorphous carbon coated copper nanowire [17]. There are also some other reports of enhanced electron emission from certain material when it is coated with amorphous carbon as compared to either of the pure material [18, 19].

Fig. 5 a, b shows the effect of inter-electrode distance on field emission properties for three different inter-electrode distance for the 4 minute deposited carbon coating PbS sample. It can be seen that the inter-electrode distance does not have a marked effect on the field emission in this case. Still 130 µm has been found to be the optimum distance for obtaining the best field emission characteristics.

4. CONCLUSIONS

Crystalline PbS nano particles of cubic in shapes have been synthesized in thin film form on both silicon and glass substrate via a simple chemical bath deposition technique. The films have been coated with amorphous carbon of different thickness by simply varying the deposition time in the dc-PECVD. The as prepared samples are characterized by XRD, FESEM, AFM and by high vacuum field emission set up. The FESEM and the AFM image confirmed that the PbS thin films have been coated with amorphous carbon. On the contrary the regarding crystallinity, the coated sample does not shows a marked changed with the thickness of the carbon coating. The coated samples showed highly improved field emission properties compared to the pure PbS thin film with turn on field as low as 3.1 V/µm. The effect of inter-electrode distance on the field emission properties has been studied in detail.

REFERENCES

1. L. Shen, Z. Chen, *Int. J. Solids Struct.* **46,** 811 (2009).
2. M. Wiora, K. Bruhne, A. Floter, P. Gluche, T.M. Willey, S.O. Kucheyevc, A.W. Van Buuren, A.V. Hamza, J. Biener, H.-J. Fecht, *Diamond Relat. Mater* **18,** 927 (2009).
3. M. Yeganeh, N. Shahtahmasebi, A. Kompany, E.K. Goharshadi, A. Youssefi, L. Siller, *Int. J. Heat Mass Tran.* **53,** 3186 (2010).
4. S.C. Lim, D.S. Lee, H.K. Choi, H. Lee, Y.H. Lee, *Diamond Relat. Mater.* **18,** 1435 (2009).
5. R.N. Gayen, A.K. Pal, *Appl. Surf. Sci.* **256,** 6172 (2010).
6. X. Zhang, L. Meng, Q. Lu, Z. Fei, P.J. Dyson, *Biomaterials* **30,** 6041 (2009).
7. Z. Yong, L. Junhua, L. Xin, Z. Changchun, *Sens. Actuators, A* **128,** 278 (2006).
8. Sk.F. Ahmed, M.K. Mitra, K.K. Chattopadhyay, *J. Phys.: Condens. Matter* **19,** 346233 (2007).
9. Sk.F. Ahmed, M.K. Mitra, K.K. Chattopadhyay, *Appl. Surf. Sci.* **253,** 5480 (2007).
10. J.F. Lin, Z.C. Wan, P.J. Wei, H.Y. Chu, C.F. Ai, *Thin Solid Films* **466,** 137 (2004).
11. Q-f Zeng, G-neng Dong, Y-bai Xie, *Appl. Surf. Sci.* **254,** 2425 (2008).
12. H. Zhu, J. Wei, K. Wang, D. Wu, *Sol. Energ. Mater. Sol. C.* **93,** 1461 (2009).
13. B.J. Jones, A. Mahendran, A.W. Anson, A.J. Reynolds, R. Bulpett, J. Franks, *Diamond Relat. Mater.* **19,** 685 (2010).
14. E.C. Rangel, E.S. de Souza, F.S. de Moraes, N.M.S. Marins, W.H. Schreiner, N.C. Cruz, *Thin Solid Films* **518,** 2750 (2010).
15. M.E. Roy, L.A. Whiteside, J. Xuc, B.J. Katerberg, *Acta Biomater.* **6,** 1619 (2010).
16. D. Banerjee, S. Mukherjee, K.K. Chattopadhyay, *Carbon* **48,** 1025 (2010).
17. B-R. Huang, C-S. Yeh, D-C. Wang, J.T. Tan, J. Sung, *New Carbon Mater.* **24(2),** 97 (2009).
18. J.J. Lia, W.T. Zheng, C.Z. Gu, Z.S. Jin, *Solid State Commun.* **132,** 253 (2004).

19. H-F. Cheng, Y-M. Tsau, T-Y. Chang, T-S. Lai, T-F. Kuo, I-N. Lin, *Diamond Relat. Mater.* **12,** 486 (2003).
20. J. Zhang, X. Jiang, *Appl. Phys. Lett.* **92,** 141108 (2008).
21. E. Pentia, L. Pintilie, I. Matei, T. Boltia, E. Ozbay, *J. Optoelectron. Adv. Mater.* **3,** 525 (2001).
22. P. Yang, C.F. Song, M.K. Lu, X. Yin, G.J. Zhou, D. Xu, D.R. Yuan, *Chem. Phys. Lett.* **345,** 429 (2001).
23. H. Hirata, K. Higoshiyama, *Bull. Chem. Soc. Jpn.* **44,** 2420 (1971).
24. P.K. Nair, M.T.S. Nair, *J. Phys. D: Appl. Phys.* **23,** 150 (1990).
25. A. Martucci, J. Fick, J. Schell, G. Battaglin, M. Guglielmi, *J. Appl. Phys.* **86,** 79 (1999).
26. C. Liu, Y.K. Kwon, J. Heo, *J. Non-Cryst. Solids* **355,** 1880 (2009).
27. S. Jana, R. Thapa, R. Maity, K.K. Chattopadhyay, *Physica E* **40,** 3121 (2008).
28. R.H. Fowler, L. Nordheim, *Proc. R. Soc. London A* **119,** 173 (1928).
29. E.L. Murphy, R.H.Jr. Good, *Phys. Rev.* **102,** 1464 (1956).
30. D. Banerjee, A. Jha, K.K. Chattopadhyay, *Appl. Surf. Sci.* **256,** 7516 (2010).
31. D. Banerjee, A. Jha, K.K. Chattopadhyay, *Physica E* **41,** 1174 (2009).